

Determination of proton strange form factors from νp elastic scattering

G. T. Garvey, W. C. Louis, and D. H. White

Los Alamos National Laboratory, Los Alamos, New Mexico 87545

(Received 12 February 1993)

A previous νp elastic scattering experiment at BNL is reanalyzed, taking into account the strange vector and axial-vector form factors of the proton F_1^s , F_2^s , and G_1^s . Values for these form factors are obtained, although with large errors due to correlations between F_1^s and F_2^s and between G_1^s and the axial vector dipole mass M_A . Future νp elastic scattering experiments could significantly improve the knowledge of these form factors.

PACS number(s): 13.15.-f, 13.15.Jr, 14.20.Dh, 25.30.Pt

I. PHYSICS MOTIVATION

It is well known, but not widely appreciated, that by way of the νp axial coupling the cross section for νp elastic scattering is sensitive to an isoscalar or singlet contribution to the proton spin. This contribution to the nucleon spin is presumably the same one responsible for the violation of the Ellis-Jaffe sum rule [1] observed in the European Muon Collaboration (EMC) measurement [2,3] of the proton spin structure function. A measurement of $\sigma(\nu p \rightarrow \nu p)$ and $\sigma(\bar{\nu} p \rightarrow \bar{\nu} p)$ carried out in the 1980s by BNL experiment 734 [4] is often cited as supporting the EMC result. This paper reanalyzes that experiment, taking account of several factors neglected in the earlier analysis.

We first briefly review the EMC result and its consequences. The EMC plus earlier SLAC experiments [2,3] measured the proton spin structure function $g_1^p(x)$ over the interval $0.01 \leq x \leq 0.7$. Using reasonable extrapolations they find

$$\int_0^1 g_1^p(x) dx = 0.126 \pm 0.01 \pm 0.015$$

at $Q^2 = 10 \text{ GeV}^2/c^2$. This differs significantly from the earlier prediction of Ellis and Jaffe (0.175 ± 0.018) [1,5], who assumed that only u (\bar{u}) and d (\bar{d}) quarks (anti-quarks) contribute to the proton spin. Taking the difference seriously leads to the conclusion that strange quarks contribute

$$\Delta s(Q^2 = 10 \text{ GeV}^2/c^2) = -0.16 \pm 0.08$$

to the proton spin where

$$\Delta q(Q^2) \equiv \int_0^1 dx [q(x, Q^2)\uparrow + \bar{q}(x, Q^2)\uparrow - q(x, Q^2)\downarrow - \bar{q}(x, Q^2)\downarrow]$$

and $q(x, Q^2)\uparrow$ (\downarrow) is the number density of quark flavor q

with momentum fraction x aligned parallel (antiparallel) to the nucleon spin. The above value of $\Delta s(Q^2)$, when coupled with nucleon and hyperon axial decay rates to fix Δu and Δd , leads to a value for the total quark spin projection along the nucleon spin direction of [5]

$$\Delta u + \Delta d + \Delta s = 0.12 \pm 0.094 \pm 0.138$$

at $Q^2 = 10 \text{ GeV}^2/c^2$. The total quark spin projection is quite small.

This rather surprising result depends on several assumptions. First, the experiment, assumed to be correct, is difficult and the effect is only at the two-sigma level. Second, extracting Δu , Δd , and Δs requires the use of SU_3 symmetry to interpret the hyperon decays. Further, the extrapolation of $g_1^p(x)$ to $x=0$ can be questioned because $g_1^p(x)$ may be more singular than assumed. There are now a number of polarized deep-inelastic-scattering measurements underway [6–8] to verify and extend the EMC measurements, but they will not remove the uncertainties confronting the interpretation of the data. It should be noted that there are alternative explanations to using strange quarks to explain the “spin anomaly.” Some theorists prefer to attribute it to gluonic contributions [9–11]. In either case the analysis presented below is valid, with only the origin of the nucleon isoscalar spin at issue.

As will be shown below, interpreting νp elastic scattering does not require SU_3 symmetry or an extrapolation to $x \rightarrow 0$ and yields Δs directly. The important role that can be played by neutrino scattering was very effectively presented by Kaplan and Manohar and Ellis and Karliner [12], though earlier work [13–15] had anticipated some of their results. The charge-changing scattering of a neutrino from a proton, $\bar{\nu}_e p \rightarrow e^+ n$, is obviously sensitive only to the isovector quark currents of the nucleon. However, neutral current scattering permits isoscalar contributions from strange or heavier quarks (and gluonic contributions in higher order). Insofar as these contributions couple through the axial current, they are contributions to the proton spin. Indeed, the neutral weak axial current of the nucleon is written as

$$\begin{aligned}
\langle N | A_\mu^Z | N \rangle &= - \left[\frac{G_F}{\sqrt{2}} \right]^{1/2} \left\langle N \left| \frac{\bar{u} \gamma_\mu \gamma_5 u - \bar{d} \gamma_\mu \gamma_5 d - \bar{s} \gamma_\mu \gamma_5 s}{2} \right| N \right\rangle \\
&= - \left[\frac{G_F}{\sqrt{2}} \right]^{1/2} \frac{(\Delta u - \Delta d - \Delta s)}{2} s_\mu \\
&= \left[\frac{G_F}{\sqrt{2}} \right]^{1/2} \left\langle N \left| -\frac{G_A(Q^2)}{2} \gamma_\mu \gamma_5 \tau_z + \frac{G_1^s(Q^2)}{2} \gamma_\mu \gamma_5 \right| N \right\rangle,
\end{aligned}$$

where $G_A(0)$ is the axial-vector coupling constant (1.256 ± 0.003), $\tau_z = +1$ (-1) for the proton (neutron), and $G_1^s(0) = \Delta s$ is the strange quark contribution to the nucleon spin. Strange quarks may also contribute to the neutral weak vector form factors, and allowance must be made for these as yet unknown effects. The effects of charmed or heavier quarks are treated as negligible [12].

Assuming no second-class currents, the complete characterization of νp and $\bar{\nu} p$ elastic scattering can be written as [4,16]

$$\frac{d\sigma}{dQ^2}(\nu p) = \frac{G_F^2}{2\pi} \frac{Q^2}{E_\nu^2} (A \pm B W + C W^2),$$

where $W = 4E_\nu/m_p - Q^2/m_p^2$, and with $\tau = Q^2/4m_p^2$,

$$A = \frac{1}{4} [G_1^2(1+\tau) - (F_1^2 - \tau F_2^2)(1-\tau) + 4\tau F_1 F_2],$$

$$B = -\frac{1}{4} G_1(F_1 + F_2),$$

$$C = \frac{1}{16} \frac{m_p^2}{Q^2} (G_1^2 + F_1^2 + \tau F_2^2).$$

G_1 , F_1 , and F_2 are the nucleon neutral weak current (NWC) axial, charge, and magnetic form factors, respectively. These NWC form factors can be written in terms of known form factors plus unknown contributions from strange quarks. Thus,

$$G_1 \equiv G_1^Z(Q^2) = \left[-\frac{G_A(Q^2)}{2} \tau_z + \frac{G_1^s(Q^2)}{2} \right].$$

The vector form factors are also written in terms of known form factors plus a strange-quark contribution:

$$F_{1,2} \equiv F_{1,2}^Z(Q^2) = \left[\left[\frac{1}{2} - \sin^2 \theta_W \right] [F_{1,2}^p(Q^2) - F_{1,2}^n(Q^2)] \tau_z - \sin^2 \theta_W [F_{1,2}^p(Q^2) + F_{1,2}^n(Q^2)] - \frac{F_{1,2}^s(Q^2)}{2} \right],$$

where $F_1^p(Q^2)$ is the electric charge (Dirac) form factor of the proton, $F_2^p(Q^2)$ is the anomalous magnetic moment (Pauli) form factor of the proton, and $F_{1,2}^s(Q^2)$ are the strange vector form factors. Using the above equation for the coupling of the proton to the Z^0 ($\tau_z = 1$) yields

$$F_{1,2}^{Z,p}(Q^2) = \left[\frac{1}{2} - 2 \sin^2 \theta_W \right] F_{1,2}^p(Q^2) - \frac{1}{2} F_{1,2}^n(Q^2) - \frac{F_{1,2}^s(Q^2)}{2}.$$

As the minimal subtraction value of $\sin^2 \theta_W = 0.2325$, the coupling of the proton to the Z^0 is dominated by the neutron's electromagnetic form factors. The values of $G_1(0)$, $F_1(0)$, and $F_2(0)$ are listed in Table I. The Q^2 dependences of the form factors are given as

$$F_{2,p}^{Z,p}(Q^2) = \frac{1.853 - 3.586 \sin^2 \theta_W + 0.956\tau / (1 + 5.6\tau)}{(1 + \tau)(1 + Q^2/M_V^2)^2} - \frac{F_2^s(Q^2)}{2},$$

$$F_{1,p}^{Z,p}(Q^2) = \frac{0.5 - 2 \sin^2 \theta_W + \tau(2.353 - 5.586 \sin^2 \theta_W) - 0.956\tau / (1 + 5.6\tau)}{(1 + \tau)(1 + Q^2/M_V^2)^2} - \frac{F_1^s(Q^2)}{2},$$

$$G_{1,p}^{Z,p}(Q^2) = \frac{-0.631}{(1 + Q^2/M_A^2)^2} + \frac{G_1^s(Q^2)}{2},$$

where $M_V = 0.843$ GeV/ c^2 , $M_A = 1.061 \pm 0.026$ GeV/ c^2 , and the neutron-electric form factor is taken as [16,17]

$$\begin{aligned}
G_E^n(Q^2) &\equiv F_1^n(Q^2) - \tau F_2^n(Q^2) \\
&= \frac{1.913\tau}{(1 + 5.6\tau)(1 + Q^2/M_V^2)^2}.
\end{aligned}$$

It is not clear what is the proper Q^2 dependence for strange form factors. If they are of dipole form at low Q^2 , it is not known what values of M_V^s and M_A^s should be used. It should also be noted that the strange form factors arise solely from sea quarks; hence, in the limit that $Q^2 \rightarrow \infty$, we would expect

TABLE I. The $Q^2=0$ values of the nucleon neutral weak form factors. $G_A(0)$ is the axial-vector coupling constant (1.256 ± 0.003). The quantities ϵ_p and ϵ_n are the electric charges of the proton and neutron, 1 and 0, respectively, while μ_p and μ_n are their anomalous magnetic moments (1.793 and -1.913) in nuclear magnetons.

$G_1(0)$	$-\frac{1}{2}G_A(0)\tau_z + \frac{1}{2}G_1^s(0)$
$F_1(0)$	$(\frac{1}{2} - \sin^2\theta_W)(\epsilon_p - \epsilon_n)\tau_z - \sin^2\theta_W(\epsilon_p + \epsilon_n)$
$F_2(0)$	$(\frac{1}{2} - \sin^2\theta_W)(\mu_p - \mu_n)\tau_z - \sin^2\theta_W(\mu_p + \mu_n) - F_2^s(0)/2$

$$F^s(Q^2)_{Q^2 \rightarrow \infty} = KQ^{-8}.$$

Jaffe [18] has taken an interesting approach to extract $F_1^s(Q^2)$ and $F_2^s(Q^2)$ by applying vector dominance and dispersion theory to the isoscalar electromagnetic form factors of the nucleon. However, we find it useful to use the same Q^2 dependence as for the nonstrange form factors:

$$F_2^s(Q^2) = \frac{F_2^s(0)}{(1+\tau)(1+Q^2/M_V^2)^2},$$

$$F_1^s(Q^2) = \frac{F_1^s(0)}{(1+\tau)(1+Q^2/M_V^2)^2},$$

$$G_1^s(Q^2) = \frac{G_1^s(0)}{(1+Q^2/M_A^2)^2},$$

where $G_1^s(0) = \Delta s$, $F_2^s(0) = \mu_s$, and $F_1^s = -\frac{1}{6}\langle r_s^2 \rangle$. Note that μ_s is the strange magnetic moment and $\langle r_s^2 \rangle = -6F_1^s(0.04 \text{ fm}^2)$ is the ‘‘strange radius’’ of the nucleon.

Before proceeding to the results of our analysis we list the principal shortcomings of the earlier analysis of E734 [4]. Specifically, we have the following. (1) The effects of strange vector form factors were not included. (2) The neutron-electric form factor $G_E^n(Q^2)$ was set to zero. (3) The value of M_A used in the earlier analysis [4] is appreciably smaller than the value extracted from the same experiment and reported in a later publication [19].

II. THE EXPERIMENT

BNL experiment 734 has been described in detail elsewhere. Briefly, the 170-metric-ton detector consisted of three major sections: (i) a modular target detector, (ii) a shower counter for longitudinal containment of electron and photon showers, and (iii) a muon spectrometer. The target detector consisted of 112 modules, where each module contained a plane of 16 liquid-scintillator cells for measuring timing and energy loss and two crossed planes of 54 proportional drift tubes for measuring position and energy loss. The fine segmentation of the elements provided determination of event topology and particle identification. 79% of the target protons were bound in carbon and aluminum, while the remaining 21% were free protons. It is important to note that for νp elastic scattering the Q^2 of the interaction is determined solely from the measurement of the proton energy, so that all protons are treated as free. The shower counter was lo-

cated downstream of the target detector and consisted of 12 radiation lengths of lead and liquid-scintillation counters. The shower counter, however, was unnecessary in the $\bar{\nu} p$ elastic-scattering analysis. The muon spectrometer was located downstream of the shower counter and consisted of a wide-aperture dipole magnet instrumented with nine proportional drift-tube pairs for measuring forward-going muons from neutrino-induced quasielastic interactions. The detector recorded all information within a $10 \mu\text{s}$ gate beginning at the alternating-gradient synchrotron (AGS) proton beam extraction.

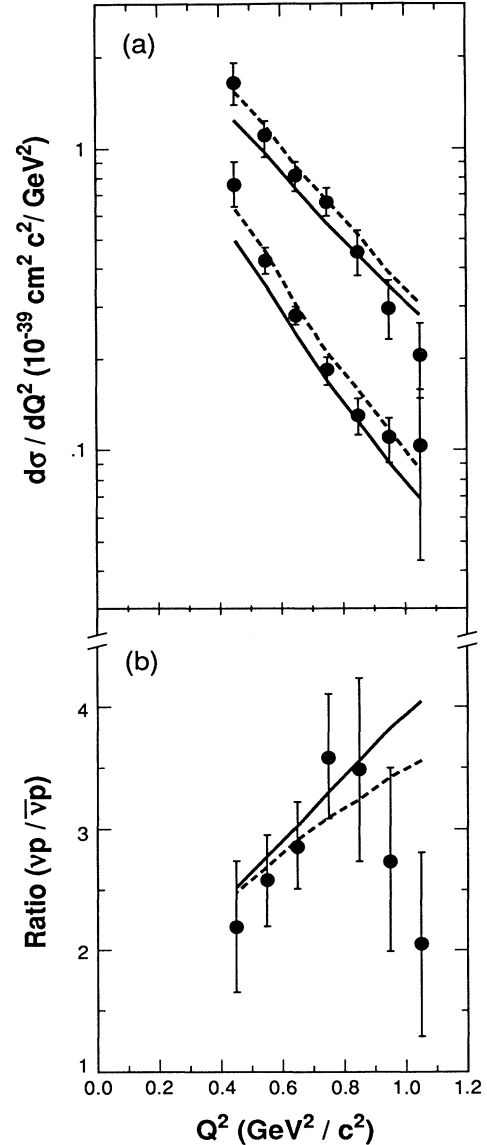


FIG. 1. (a) The measured νp and $\bar{\nu} p$ elastic-scattering differential cross sections from experiment 734 at Brookhaven [4]. (b) The ratio of measured νp and $\bar{\nu} p$ elastic-scattering differential cross sections from experiment 734. The solid and dashed curves correspond to fits I and IV, which are discussed in the text. The errors correspond to statistical and Q^2 -dependent systematic errors added in quadrature and do not include Q^2 -independent systematic errors.

The horn-focused wide-band neutrino beam resulted from 28-GeV protons incident on a production target creating pions and kaons. The pions and kaons subsequently decayed in flight to beams of ν_μ (positive horn focus) and $\bar{\nu}_\mu$ (negative horn focus) with mean energies of 1.3 and 1.2 GeV, respectively. By measuring muons from quasielastic scattering in the magnetic spectrometer, the fraction of antineutrino contamination in the neutrino beam was determined to be 0.024 ± 0.005 , while the neutrino contamination in the antineutrino beam was determined to be 0.087 ± 0.013 .

Data were acquired in separate exposures of 0.55×10^{19} protons (positive focused beam) and 2.5×10^{19} protons (negative focused beam) on the production target. These exposures resulted in total data samples of 5.5×10^5 neutrino events and 2.5×10^6 antineutrino events. After a complete data analysis and background subtraction, the final numbers of νp and $\bar{\nu} p$ elastic events were determined to be 951 and 776, respectively. The corresponding numbers of $\nu n \rightarrow \mu^- p$ and $\bar{\nu} p \rightarrow \mu^+ n$ quasielastic events, which were used for normalization, were 11 677 and 20 546, respectively. The measured νp and $\bar{\nu} p$ elastic-scattering differential cross sections are shown in Fig. 1(a) and the measured ratios in Fig. 1(b). The error bars represent statistical and Q^2 -dependent systematic errors, which have been added in quadrature. In addition, there were Q^2 -independent systematic errors, which correspond to scale uncertainties in the absolute cross sections, of 11.2% and 10.4% for νp and $\bar{\nu} p$, respectively. The positive correlation coefficient between these Q^2 -independent systematic errors was determined to be 0.50.

III. FITTING PROCEDURE AND RESULTS

The data of Fig. 1(a) were fit to the cross-section form discussed above by using the MINUIT computer program to minimize the χ^2 . In particular,

$$\chi^2 = \sum_{\nu} \frac{(\sigma_i^f - \sigma_i^d/s_\nu)^2}{\delta\sigma_i^2} + \sum_{\bar{\nu}} \frac{(\sigma_i^f + \sigma_i^d/s_{\bar{\nu}})^2}{\delta\sigma_i^2} + \frac{(1 - s_\nu s_{\bar{\nu}})^2}{0.153^2} + \frac{(1 - s_\nu/s_{\bar{\nu}})^2}{0.108^2} + \frac{(M_A - 1.061)^2}{0.026^2},$$

where the sums are over all seven νp and seven $\bar{\nu} p$ data points. In the expression above, σ_i^f are the fitted differential cross sections, σ_i^d are the measured differential cross sections, s_ν and $s_{\bar{\nu}}$ are the fitted scale factors for the neutrino and antineutrino data points, $\delta\sigma_i$ are the statistical and Q^2 -dependent errors added in quadrature, 0.153 and 0.108 are the Q^2 -independent total

errors and correlated errors, and 1.061 ± 0.026 GeV/ c^2 is the present world average for the axial-vector dipole mass. Six quantities, in general, are determined: the scale factors s_ν and $s_{\bar{\nu}}$, the axial-vector dipole mass M_A , and the strange form factors G_1^s , F_1^s , and F_2^s . Also, the present world average of $\sin^2\theta_W = 0.2325$ is used in the above cross-section expressions.

The results of the fits are shown in Table II. For the first fit (solid curves in Fig. 1) all strange form factors, G_1^s , F_1^s , and F_2^s , were set to zero, and a satisfactory χ^2 was obtained by letting M_A increase to 1.086 ± 0.015 (in fact, all the χ^2 in the fits below are too small, suggesting that the errors were overestimated in the experiment). It is perhaps worthwhile to point out that the value reported for M_A ($= 1.09 \pm 0.03 \pm 0.02$) from experiment 734 in a later publication [19] is larger than but consistent with the world average. The second fit shows, however, that the χ^2 is reduced by allowing G_1^s to become negative and keeping F_1^s and F_2^s fixed to zero with M_A dropping to 1.049 ± 0.007 . A negative G_1^s increases both the νp and $\bar{\nu} p$ elastic cross sections, and, therefore, there is a strong correlation between the fits for G_1^s and M_A because a larger value of M_A also increases the cross sections at higher Q^2 . All of the errors in Table II take into account these and other correlations. The third fit allows F_1^s to float to a positive value and F_2^s to a negative value. There is a correlation between the two strange vector form factors because a positive value for either decreases the νp elastic cross section and increases the $\bar{\nu} p$ cross section, or, in other words, F_1^s and F_2^s are determined by the difference in the νp and $\bar{\nu} p$ measured cross sections while G_1^s is determined by the sum of the measured cross sections. Nevertheless, the data prefer F_1^s to be positive, which, in the formulation discussed above, causes the νp cross section to turn down and the $\bar{\nu} p$ cross section to turn up at higher Q^2 (see Fig. 1). This behavior has also been observed in a previous νp elastic-scattering experiment [20].

Finally, the fourth fit (dashed curves in Fig. 1) is the same as the third fit but with

$$M_A = 1.032 \pm 0.036 \text{ GeV}/c^2,$$

which was the world average prior to the E734 result. This lower value for M_A leads, as expected, to a greater negative value for G_1^s and a better χ^2 for the fit. We have also tried higher powers of Q^2 and larger masses for the strange form factor Q^2 dependences without changing the fits appreciably. The coefficients change, but the values of the strange form factors at the Q^2 of the experi-

TABLE II. The fit results for the strange form factors $G_1^s(0) = \Delta s$, $F_1^s = -\frac{1}{6}\langle r_s^2 \rangle$, and $F_2^s(0) = \mu_s$, and the axial-vector dipole mass M_A .

Fit	$G_1^s(0)$	F_1^s	$F_2^s(0)$	M_A	χ^2/N_{DOF}
I	0	0	0	1.086 ± 0.015	14.12/14
II	-0.15 ± 0.07	0	0	1.049 ± 0.019	9.73/13
III	-0.13 ± 0.09	0.49 ± 0.70	-0.39 ± 0.70	1.049 ± 0.023	9.28/11
IV	-0.21 ± 0.10	0.53 ± 0.70	-0.40 ± 0.72	1.012 ± 0.032	8.13/11

ment ($0.4 < Q^2 < 1.1 \text{ GeV}^2/c^2$) remain the same.

Thus, while very interesting, E734 is not decisive in determining any of the strange form factors. The value of $G_1^s(0)$ is strongly correlated to the value of M_A and the number of protons that one assumes to be available for quasielastic scattering in ^{12}C . Satisfactory fits are obtained for values for G_1^s that range from 0 to -0.21 ± 0.10 , depending on how M_A is dealt with. The strange vector form factors $F_1^s(Q^2)$ and $F_2^s(Q^2)$ are seen to be correlated and are consistent with zero. However, the very different Q^2 behavior of $d\sigma/dQ^2(\nu p)$ compared to $d\sigma/dQ^2(\bar{\nu} p)$ seems to favor $F_1^s(Q^2) > 0$ and $F_2^s(Q^2) < 0$. These signs are expected if there are hyperon plus kaon configurations in the nucleon. Note that once $F_2^s(0)$ is measured elsewhere (e.g., by the SAMPLE experiment [21]), then F_1^s can be determined with fairly good precision. In fit IV, for example, the sum $F_1^s + F_2^s(0)$ is fit to be 0.13 ± 0.22 .

It appears that better νp elastic data in this Q^2 range

would be most interesting. The LSND experiment at LAMPF [22] should be able to fix $G_1^s(0)$ without the uncertainties mentioned above because $Q^2 \leq 0.09 \text{ GeV}^2/c^2$. It would be essential for any new experiment in the same Q^2 regime as E734 to also measure charge-changing quasielastic scattering, for which the $Q^2=0$ values for all form factors are known and fits to the data should allow the determination of M_A appropriate for the analysis of the neutral current events. In addition to learning about strange-quark contributions to the properties of the nucleon, it should be informative to obtain information about the Q^2 dependence of form factors that arise solely from sea-quark contributions.

ACKNOWLEDGMENTS

We thank C. Benesh, T. Goldman, R. L. Jaffe, W. Marciano, and R. McKeown for stimulating discussions.

-
- [1] J. Ellis and R. L. Jaffe, Phys. Rev. D **9**, 1444 (1974); **10**, 1669 (1974).
 - [2] J. Ashman *et al.*, Phys. Lett. B **206**, 364 (1988).
 - [3] J. Ashman *et al.*, Nucl. Phys. B **328**, 1 (1989).
 - [4] L. A. Ahrens *et al.*, Phys. Rev. D **35**, 785 (1987).
 - [5] R. L. Jaffe and A. Manohar, Nucl. Phys. **B337**, 509 (1990). We use the values of Δs and $\Delta u + \Delta d + \Delta s$ quoted in this paper. The slight differences arise from the F and D values extracted from hyperon decay.
 - [6] CERN Experiment NA47 (SMC) (unpublished).
 - [7] SLAC Experiments E142 and E143 (unpublished).
 - [8] HERMES Experiment at HERA (unpublished).
 - [9] A. V. Efremov and O. V. Teryaev, JINR Dubna Report No. JINR EZ-88-297, 1988 (unpublished).
 - [10] G. Alterelli and G. G. Ross, Phys. Lett. B **212**, 391 (1988).
 - [11] R. D. Carlitz, J. C. Collins, and A. H. Mueller, Phys. Lett. B **214**, 229 (1988).
 - [12] D. Kaplan and A. Manohar, Nucl. Phys. **B310**, 527 (1988); J. Ellis and M. Karliner, Phys. Lett. B **213**, 73 (1988).
 - [13] J. Collins, F. Wilczek, and A. Zee, Phys. Rev. D **18**, 242 (1978).
 - [14] R. N. Mohapatra and G. Senjanović, Phys. Rev. D **19**, 2165 (1979).
 - [15] L. Wolfenstein, Phys. Rev. D **19**, 3450 (1979).
 - [16] E. Beise and R. McKeown, Commun. Nucl. Part. Phys. **20**, 105 (1991).
 - [17] S. Platchkov *et al.*, Nucl. Phys. **A508**, 343 (1990).
 - [18] R. L. Jaffe, Phys. Lett. B **229**, 275 (1989).
 - [19] L. A. Ahrens *et al.*, Phys. Lett. B **202**, 284 (1988).
 - [20] J. Horstkotte *et al.*, Phys. Rev. D **25**, 2743 (1982).
 - [21] Bates Experiment No. 89-06 (SAMPLE) (unpublished).
 - [22] LAMPF Experiment No. 1173 (LSND) (unpublished).